

New iridium and rhodium chiral di-*N*-heterocyclic carbene (NHC) complexes and their application in enantioselective catalysis†

Matthew S. Jeletic, Muhammad T. Jan, Ion Ghiviriga, Khalil A. Abboud and Adam S. Veige*

Received 3rd November 2008, Accepted 30th January 2009

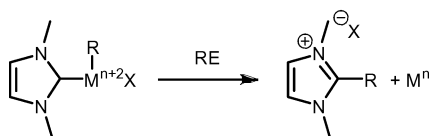
First published as an Advance Article on the web 23rd February 2009

DOI: 10.1039/b819524b

New iridium and rhodium complexes prepared from C_2 -symmetric *trans*-9,10-dihydro-9,10-ethanoanthracene-11,12-bis(1-*R*)-benzimidazolidine-2-ylidene ligands ($R = \text{Me}$, ^iPr , and dPh) have been synthesized and characterized. Their catalytic activities have been tested in enantioselective hydrogenation and hydroformylation reactions. The ee's for the reactions are low. Evidence indicates that even chelating di-*N*-heterocyclic carbene ligands are susceptible to reductive elimination.

Introduction

N-Heterocyclic carbenes (NHCs) function as ligands in a broad scope of metal-catalyzed organic transformations.^{1–10} Though versatile ligands, much of the excitement is due to their unparalleled success in Grubbs' second-generation olefin metathesis catalyst.^{2,11–13} Grubbs' swap of a trialkylphosphine ligand for a bulky NHC has inspired numerous additional advances in catalysis. In particular, (NHC)Pd catalysts exhibit high activity and selectivity in cross-coupling reactions.⁵ However, the PR_3/NHC switch is not yet a general recipe for enhanced reactivity. For example, alkene hydrogenation with monodentate NHC complexes yields modest results compared to analogous phosphorous-based catalysts.^{14–27} The Achilles heel in (NHC)M-catalyzed hydrogenation is the tendency for NHC reductive elimination (RE) to the imidazolium salt $[\text{NHC-H}]^+$ (Scheme 1). Not surprisingly, there is to date only a single example of enantioselective alkene hydrogenation using chiral monodentate NHC complexes.¹⁹



Scheme 1 General reductive elimination pathway (RE).

The decomposition pathway is not limited to C–H bond elimination. In 1998, Cavell *et al.* demonstrated $[(1,3\text{-Me-NHC})\text{-Pd}(\text{Me})\text{cod}]^+$ (where 1,3-Me-NHC = 1,3-dimethyl-imidazol-2-ylidene) decomposes into the 1,2,3-trimethylimidazolium salt (1,3-MeNHC-Me⁺), Pd⁰ and free 1,5-cyclooctadiene (cod).²⁸ Two years later, McGuinness and Cavell treated $[(\text{TMIY})\text{Pd}(\text{Me})\text{Cl}]_2$ (TMIY = 1,3,4,5-tetramethyl-imidazol-2-ylidene) with AgBF_4 and CO at -50°C , then warmed the mixture to -20°C . The

observed major and minor products were the acylimidazolium and methylimidazolium salts, respectively.²⁹

Over the next decade mounting experimental^{28–40} and theoretical^{41–45} evidence implicates reductive elimination as a major catalyst decomposition pathway for NHC complexes. Van Rensburg *et al.* observed C–H reductive elimination of the imidazolium salt $[\text{IMes-H}]^+$ from $[(\text{IMes})\text{Co}(\text{CO})_3]_2$ under hydroformylation conditions.^{37,38} This decomposition pathway is not exclusive to the late transition metals, considering Bullock *et al.* demonstrated IMes reductively eliminates from $[\text{Cp}(\text{IMes})\text{W}(\text{CO})_2]\text{-}[\text{B}(\text{C}_6\text{F}_5)_4]$ as $[\text{IMes-H}][\text{B}(\text{C}_6\text{F}_5)_4]$ during ketone hydrogenation.⁴⁰

Cavell, Yates *et al.* computationally explored some factors that prevent NHC reductive elimination.^{31,41–45} The activation barrier to reductive elimination increases by 5.6 kcal mol⁻¹ when the *N*-alkyl substituent changes from $\text{Cl} < \text{H} < \text{Ph} < \text{Me} < \text{Cy} < ^i\text{Pr} < \text{Np} < ^t\text{Bu}$. Electron-donating *N*-substituents make the Pd–C(NHC) bond more resilient toward reductive elimination, and *vice versa* for electron-withdrawing groups.⁴³ Changes in the carbene twist angle show only small changes in the reductive elimination activation energies due to a cancelling effect. As the carbene twist angle increases from 15° to 90° the relative barriers to reductive elimination decrease, but the ground state energies also decrease due to steric relief.⁴⁴ In a model system, calculations indicate the angle between two PMe_3 spectator ligands, opposite the NHC, is inversely proportional to the reductive elimination activation energy. From these studies, Cavell, Yates *et al.* note that using chelating NHC ligands will impede reductive elimination.

One type of chelating ligand is the so-called mixed-NHC that chelates through the NHC and an additional donor moiety. These ligands are effective for hydrogenation, including highly desirable enantioselective versions.^{2,46–56} In the same manner, di-NHC ligands are expected to be resilient to reductive elimination but there are no reports for hydrogenation of alkenes.

We report the synthesis of C_1 -symmetric chiral chelating di-NHC iridium and rhodium complexes. The new iridium complexes complement our previous synthesis⁵⁷ of rhodium derivatives and together enable a meaningful comparison of (NHC)M stability. Fig. 1 displays the ligand architecture featured in this study. This report will show that even chelating di-NHC ligands are susceptible to reductive elimination under hydrogenation and hydroformylation conditions.

Center for Catalysis, Department of Chemistry, University of Florida, P.O. Box 117200, Gainesville, Florida, 32611, USA. E-mail: veige@chem.ufl.edu; Fax: +1 352-392-9844; Tel: +1 352-392-9844

† Electronic supplementary information (ESI) available: Multi-nuclear NMR and 2D NMR spectra, IR spectra, and X-ray crystallographic data. CCDC reference numbers 707708 and 707709. For ESI and crystallographic data in CIF or other electronic format see DOI: 10.1039/b819524b

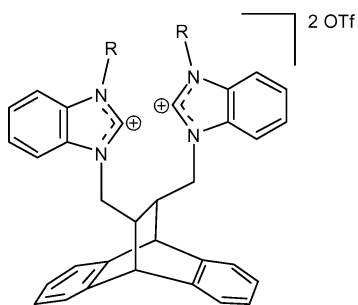


Fig. 1 Chiral di-NHC ligand precursor based on the *trans*-9,10-dihydro-9,10-ethanoanthracene backbone.

Results and discussion

Synthesis and characterization of [(DEAM-diPhBY)Ir(cod)](OTf) (**3-diPh**) and [(DEAM-IBY)Ir(cod)](OTf) (**3-ⁱPr**)

In accordance with Cavell's study we sought a large *N*-alkyl substituted NHC. **1**-Diphenylmethanebenzimidazole (**1-diPh**) is synthesized in 63% yield by treating benzimidazole with chlorodiphenylmethane in xylenes, KOH and a catalytic amount of ⁿBu₄NBr.^{58,59} The synthesis of **1-isopropylbenzimidazole** (**1-ⁱPr**) is reported elsewhere.⁶⁰ Though **1-diPh** is available commercially, it is exorbitantly expensive. Our spectroscopic studies and combustion analysis confirm the identity of **1-diPh**. The diagnostic diphenylmethine resonance on **1-diPh** shifts downfield to 6.97 ppm from 6.12 ppm for chlorodiphenylmethane, and the ¹³C{¹H} spectrum matches the published data.⁵⁹

Scheme 2 depicts the route for synthesizing the iridium complexes [(DEAM-diPhBY)Ir(cod)](OTf) (**3-diPh**) and [(DEAM-IBY)Ir(cod)](OTf) (**3-ⁱPr**). Attaching **1-R** to the *trans*-9,10-dihydro-9,10-ethanoanthracene backbone by straightforward triflate⁵² substitution cleanly provides (DEAM-diPhBI)(OTf)₂ (**2-diPh**) and (DEAM-IBI)(OTf)₂ (**2-ⁱPr**)⁶¹ as white powders in 75% and 95% yield, respectively.

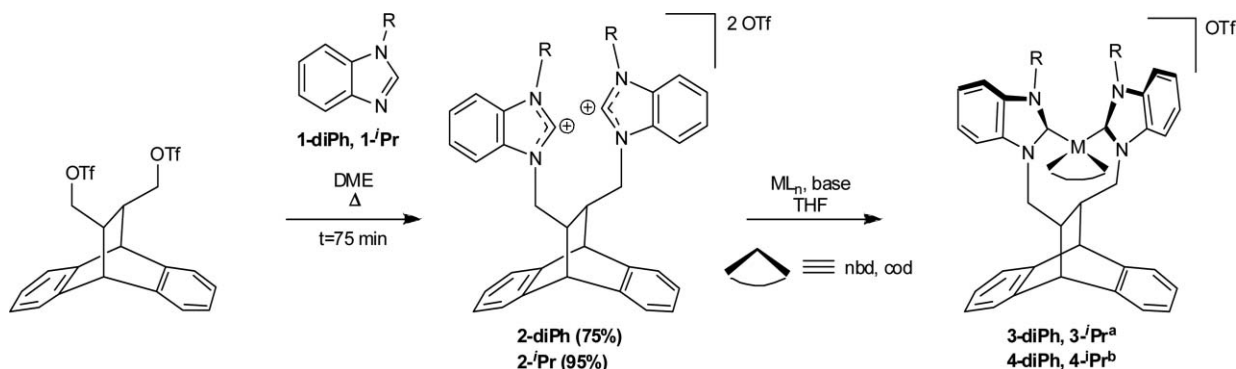
Common spectroscopic and combustion techniques elucidate the identity and purity of **2-diPh**. The ¹H NMR spectrum of **2-diPh** reveals a characteristic benzimidazolium salt C-2 proton resonance at 9.27 ppm. Aromatic protons from the phenyl groups obscure the location of the diphenylmethine resonance. The ¹H NMR and ¹³C{¹H} NMR spectra routinely reveal that exactly one

molecule of DME is present after standard work up procedures. If desired, the DME can be removed by heating under vacuum for five days, though its removal prior to metalation is not necessary.

The iridium complexes **3-diPh** and **3-ⁱPr** were prepared from the corresponding **2-R** and (acac)Ir(cod) in THF. Though the reaction is performed under an inert atmosphere, the complexes are isolated on the bench top as air- and moisture-stable orange powders in 89% (**3-diPh**) and 99% (**3-ⁱPr**) yield. The ¹H NMR spectrum of **3-diPh** reveals an intricate pattern of resonances, attributable to a C₁-symmetric complex. The spectrum displays two distinct bridgehead proton resonances at 4.41 and 4.99 ppm, due to the lowered symmetry. One of the diphenylmethine protons is located at 8.38 ppm but the second proton is indistinguishable from nearby aromatic protons. The ¹³C{¹H} NMR spectrum exhibits two prominent resonances at 189.8 and 186.9 ppm, corresponding to the carbene carbons. The iridium-bound cod carbons resonate at 72.3, 75.1, 81.3 and 85.8 ppm.

Spectroscopic ¹H NMR data for **3-ⁱPr** show a large number of resonances, indicating the complex is again C₁-symmetric. Some of the more recognizable signals include the *isopropyl* methines as septets at 5.05 and 6.23 ppm. The four corresponding *isopropyl* methyls resonate as doublets at 0.91, 1.66, 1.80 and 2.02 ppm. The ¹³C{¹H} NMR spectrum displays signals at 188.1 and 183.8 ppm attributable to the carbene carbons; the four cod olefinic carbons resonate at 69.2, 75.3, 79.1 and 85.6 ppm.

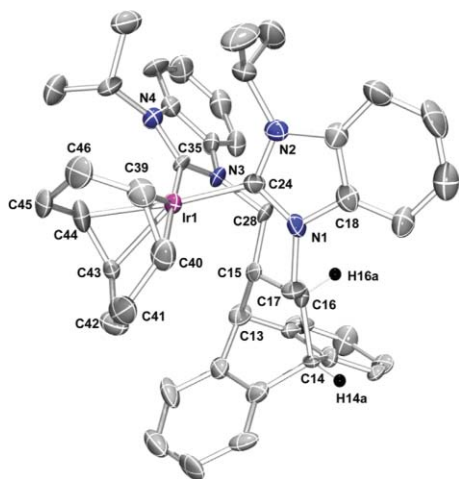
A single-crystal X-ray diffraction experiment conducted on **3-ⁱPr** agrees with the spectroscopically determined C₁ symmetry (Fig. 2). Table 1 lists selected bond lengths, bond angles and torsion angles.⁶² The asymmetric unit consists of two crystallographically independent molecules in the *Pn* space group. The DEAM and cod ligands coordinate *cis* to the iridium center to generate a square-planar geometry (e.g. ∠C40–Ir1–C44 = 89.8(6)°). The Ir–C(NHC) bond lengths are 2.056(9) and 2.081(10) Å. Herrmann *et al.* report a similar complex (NHC)Ir(cod)Cl, with an Ir–C(NHC) bond length of 2.022(7) Å.⁶³ Shi *et al.* report shorter Ir(III)–C(NHC) bond lengths for the BINAP–NHC ligand (1.996(8) and 2.001(8) Å), where the NHC is a 1-methylbenzimidazolidine-2-ylidene, reflecting the difference between Ir^I and Ir^{III}.⁶⁴ The two different Ir–C(NHC) bond lengths in **3-ⁱPr**, though subtle, reflects the ~12° difference in the carbene twist angles of the two heterocycles. The average torsion angle between the hydrogen atoms (H13–H15 and H14–H16) attached



Scheme 2 Synthesis of [(DEAM-RBY)Ir(cod)](OTf) and [(DEAM-RBY)Rh(nbd)](OTf) (R = diPh, ⁱPr). Conditions: (a) M = (acac)Ir(cod), base = Cs₂CO₃, *t* = 16 h, *T* = 23 °C, yield; R = ⁱPr (99%) R = diPh (89%), (b) M = [Rh(nbd)₂](BF₄), base = KN(Si(CH₃)₃)₂, *t* = 16 h, *T* = –35 °C, yield; R = ⁱPr (92%) R = diPh (88%).

Table 1 Selected bond lengths, bond angles, and torsion angles for **3-Pr**

Bond lengths/Å	
Ir(1)–C(24)	2.056(9)
Ir(1)–C(35)	2.081(10)
Ir(1)–C(39)	2.165(10)
Ir(1)–C(43)	2.172(9)
Ir(1)–C(40)	2.228(11)
Ir(1)–C(44)	2.229(10)
N(1)–C(17)	1.477(11)
N(1)–C(24)	1.355(11)
N(2)–C(25)	1.503(12)
Bond angles/°	
C(40)–Ir(1)–C(44)	89.8(5)
C(43)–Ir(1)–C(44)	37.4(4)
N(1)–C(24)–N(2)	107.3(8)
N(2)–C(25)–C(26)	107.9(8)
N(1)–C(17)–C(16)	112.3(8)
Torsion angles/°	
N(2)–C(24)–Ir(1)–C(35)	72
N(3)–C(35)–Ir(1)–C(24)	60
H(13)–C(13)–C(15)–H(15)	71
H(14)–C(14)–C(16)–H(16)	70

**Fig. 2** Molecular structure of **3-Pr**. Thermal ellipsoids are shown at the 50% probability level and the OTf counter ion is removed for clarity.

to the bridge and bridgehead carbons is $\sim 70^\circ$. This is noteworthy because the coupling constant between these protons, determined by ^1H NMR spectroscopy, is 0 Hz and is consistent with Karplus theory.⁶⁵

Synthesis and characterization of [(DEAM-diPhBY)Rh(nbd)]-(OTf) (**4-diPh**), [(DEAM-IBY)Rh(nbd)](OTf) (**4-Pr**) and [(DEAM-MbBI)Rh(CO)₂](BF₄) (**5-Me**)

The rhodium complexes [(DEAM-diPhBY)Rh(nbd)](OTf) (**4-diPh**) and [(DEAM-IBY)Rh(nbd)](OTf) (**4-Pr**) were synthesized according to Scheme 2. In the metalation step the di-NHC is generated *in situ* by deprotonating the dibenzimidolium triflate salt with $\text{KN}(\text{Si}(\text{CH}_3)_2)_2$ at -35°C . **4-diPh** and **4-Pr** were prepared from monometallic $[\text{Rh}(\text{nbd})_2](\text{BF}_4)$ at -35°C . Like the

iridium complexes, the rhodium versions are prepared in an inert atmosphere, but isolated on the bench top as air- and moisture-stable golden yellow powders in 88% (**4-diPh**) and 92% (**4-Pr**) yield. The ^1H NMR and $^{13}\text{C}\{^1\text{H}\}$ NMR spectra demonstrate the rhodium complexes are C_1 -symmetric in solution.

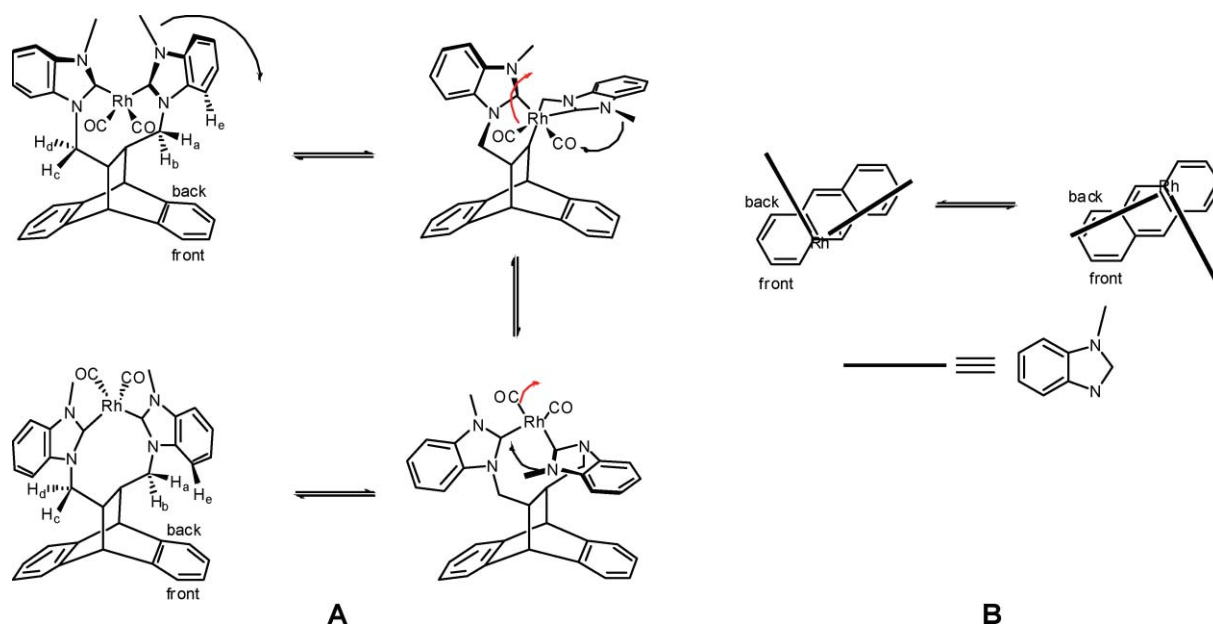
In particular, the ^1H NMR spectrum of **4-Pr** exhibits diagnostic *isopropyl* methine septet resonances at 5.30 and 6.34 ppm, and doublets for the *isopropyl* methyls at 1.39, 1.60, 1.86 and 1.94 ppm. The distinct diastereotopic nbd bridge protons appear at 1.39 and 1.41 ppm. The $^{13}\text{C}\{^1\text{H}\}$ NMR spectrum displays doublet signals at 192.1 and 191.9 ppm attributable to the carbene carbons; the four nbd olefinic carbons resonate as doublets at 65.1, 70.6, 74.5 and 80.3 ppm. In addition, the nbd bridge carbon resonance appears at 67.8 ppm. High-resolution mass spectrometry reveals the actual (m/z 745.2782) and theoretical (m/z 745.2772) M^+ parent ion values match.

4-diPh is characterized by multinuclear NMR and high-resolution mass spectrometry. The ^1H NMR spectrum of **4-diPh** reveals diagnostic diphenylmethine signals at 7.24 and 8.53 ppm; the ethanoanthracene bridgehead protons resonate at 4.35 and 5.00 ppm. The nbd methylene protons are diastereotopic and resonate at 1.19 and 1.23 ppm as doublets. The olefinic nbd and NHC carbons in the $^{13}\text{C}\{^1\text{H}\}$ NMR spectrum are identified by their doublet multiplicity at 67.3, 70.7, 75.4, 80.9 ppm and 194.9, 194.7 ppm, respectively. The nbd bridge (68.05 ppm) and diphenylmethine (68.6, 68.8 ppm) resonances were identified by a 2D-gHMOC experiment. The high-resolution mass spectrometry experiment demonstrates the actual (m/z 993.3398) and theoretical (m/z 993.3399) M^+ parent ion values are nearly identical.

The dicarbonyl complex [(DEAM-MBY)Rh(CO)₂](BF₄) (**5-Me**) is synthesized by treating **4-Me**⁵⁷ with 100 bar of CO at 50°C for 24 h. Complex **5-Me** is isolated as a yellow powder in 92% yield. The ^1H NMR spectrum clearly shows a decrease in the number of signals, signifying the substitution of CO for nbd. The $^{13}\text{C}\{^1\text{H}\}$ NMR spectrum confirms substitution of nbd with the disappearance of the nbd olefinic resonances and the emergence of two doublets at 179.9 and 180.0 ppm, corresponding to two CO ligands. The carbene carbons resonate downfield as doublets at 185.6 and 186.3 ppm. The IR spectrum of **5-Me** complements the NMR spectral studies and confirms the presence of two CO groups. The stretching frequencies are 2025.8 and 2083.6 cm^{-1} and fall within the normal range for Rh(NHC)CO complexes.^{66–69}

Several 2D experiments, gDQCOSY, gHMOC, gHMBC and NOESY, allow for the absolute assignment of all carbon and proton signals. The NOESY spectrum at 25°C taken with a mixing time of 1 s displays several exchange cross peaks between protons with similar connectivity but different stereochemistry, e.g. H_a , H_b or H_c , H_d . Of the two methylene protons (H_c , H_d) on the corresponding carbon, the one with two large coupling constants, therefore *anti*-periplanar to H_a , exchanges with the proton (H_b) exhibiting only one large coupling constant on the corresponding carbon. At -15°C the exchange rate is negligible and the unique carbon and proton signals are unequivocally assigned *via* an NOE difference experiment (see electronic supplementary information (ESI) for full details†). The exchange rates at higher temperatures imply **5-Me** is fluxional.

Scheme 3 depicts the proposed ring inversion which is best described as a degenerate isomerism. In the first step, one of the



Scheme 3 Proposed mechanism for the degenerate isomerization of **5-Me**. B: Top view of the degenerate isomerization.

benzimidazole rings moves into a parallel position with respect to the anthracene backbone. The rhodium center then moves upwards. Finally, the rhodium moves to the opposite side of the backbone and the benzimidazole ring swings back into a perpendicular position. Notice that the H_c proton exchanges in space relative to the backbone *via* the degenerate isomerization. As well, the methylene protons (H_a and H_b) exchange stereochemical positions. This mechanism is consistent with a NOE difference experiment in which the exchange rates were determined at 5, 25 and 45 °C. The barrier to ring inversion is calculated as $16.9 \pm 1.8 \text{ kcal mol}^{-1}$ (see ESI for the full details[†]). More importantly, $\Delta S^\ddagger = -7 \pm 6 \text{ cal mol}^{-1} \text{ K}^{-1}$ and is also consistent with the proposed mechanism. At the transition state, one imidazole must align parallel to the backbone. A small and negative entropy of activation fits the increased order at the transition state. However, the data used to create the Eyring plot is marred by interference by additional NOE's and inherent errors associated with temperature accuracy. Thus, the ΔS^\ddagger interpretation is made cautiously.

The substitution of norbornadiene for CO is further supported by an X-ray crystallographic experiment. Fig. 3 depicts the molecular structure of **5-Me** and Table 2 lists selected bond lengths and bond angles. The asymmetric unit consists of two crystallographically independent molecules in the $P2(1)/c$ space group. The NHCs coordinate in a *cis* fashion along with *cis* carbonyls to complete a square-planar geometry. The Rh–C(NHC) bond lengths are 2.063(3) and 2.078(4) Å and are comparable to other Rh–C (benzimidazole–NHC) bond lengths reported by Shi *et al.*^{64,70,71} The Rh–C(CO) bond lengths are 1.874(5) and 1.897(4) Å and are consistent with analogous Rh(CO)(NHC) complexes.^{66,67,72,73}

Olefin hydrogenation

3-R and **4-R** were evaluated as catalysts for the hydrogenation of *trans*-methylstilbene, methyl-2-acetamidoacrylate and benzene. Recall the objective is to not only determine activity but to

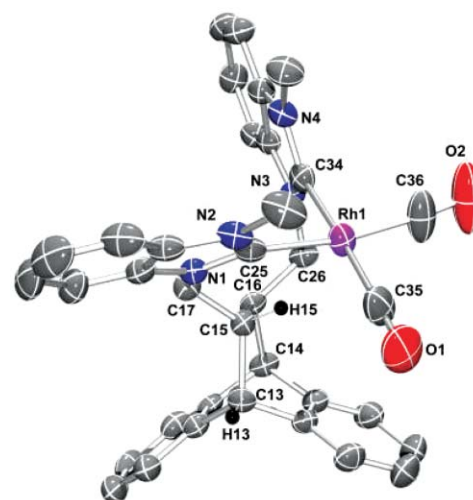
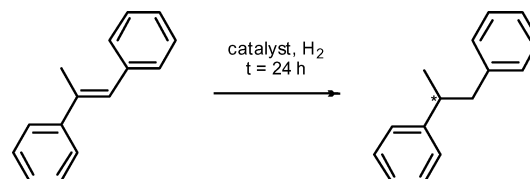


Fig. 3 Molecular structure of **5-Me**. Thermal ellipsoids are shown at the 50% probability level and the BF_4 counter ion is removed for clarity.

conclusively show the chelating di-NHC is resistant to reductive elimination. *trans*-Methylstilbene is a difficult substrate to hydrogenate and is chosen to assess the limits of the catalysts (Scheme 4). Table 3 summarizes the results.



Scheme 4 Catalytic hydrogenation of *trans*-methylstilbene.

Using **4-Me** as the catalyst, the conversion is greater than 98%, however a black material precipitates from solution during the course of the reaction. Clearly, decomposition of **4-Me** occurs

Table 2 Selected bond lengths and bond angles for **5-Me**

Bond lengths/Å	
Rh(1)–C(36)	1.874(5)
Rh(1)–C(35)	1.897(4)
Rh(1)–C(34)	2.063(3)
Rh(1)–C(25)	2.078(4)
C(35)–O(1)	1.132(5)
C(36)–O(2)	1.122(5)
N(4)–C(34)	1.344(4)
N(4)–C(33)	1.468(4)
Bond angles/°	
Rh(1)–C(36)–O(2)	175.2(6)
C(36)–Rh(1)–C(35)	94.23(19)
C(25)–Rh(1)–C(35)	89.34(16)
C(25)–Rh(1)–C(34)	90.19(13)
N(4)–C(34)–N(3)	106.3(3)
C(34)–Rh(1)–C(35)	176.40(17)

and one possibility is the formation of Rh^0 . Rh^0 and Ir^0 species, whether colloidal or nanoparticles, are well known to hydrogenate alkenes, even unactivated tetrasubstituted substrates. Since these ligands are chiral, any product enantioselectivity is evidence that the ligand remains bound during catalysis, but using (*S*)-**4-Me** as the catalyst (entry 2) provides no optical induction (0% ee). This raises questions as to the true identity of the active catalyst and the fate of the NHC ligand during the reaction.

Mercury poisoning is a common method to test for M^0 species. However, there are inherent flaws associated with Hg^0 poisoning. Mercury does not form an amalgam with Rh^0 and Ir^0 , as with Pd^0 , and therefore poisoning these species is more difficult.⁷⁴ In fact, the results from entries 3–6 demonstrate Hg^0 sequestration produces inconsistent results. For instance, compare entries 3 and 4. Though every parameter was held constant the conversion changes from 21 to 100%. The only rational explanation is a difference in stir rate. Though the stir settings were the same in both, the stir bar may not stir evenly during each experiment, resulting in uneven Hg^0 distribution throughout the reaction vessel. In another experiment, adding additional Hg^0 (1.86 g) resulted in no conversion. The key point is though it appears Rh^0 may be the active catalyst, Hg^0 poisoning alone is not sufficient evidence.

As a control experiment $[\text{Rh}(\text{nbd})_2](\text{BF}_4)$, the precursor to **4-Me**, was tested for hydrogenation of *trans*-methylstilbene (entry 7). Full conversion to the alkane product and a black precipitate is observed, but when Hg^0 is added the conversion drops to zero (entry 8). Using similar conditions both $[\text{Rh}(\text{nbd})_2](\text{BF}_4)$ and **4-Me** generate a catalyst capable of hydrogenating benzene. Rh^I precursors are well known to break down into Rh^0 species that are excellent catalysts for benzene hydrogenation.⁷⁵ These results point to a common Rh^0 as the active catalyst.

As mentioned above, one route to Rh^0 is NHC reductive elimination to the corresponding imidazolium salt. The observation of black precipitates prompted a closer investigation of the reaction mixture after hydrogenation. Indeed, a ^1H NMR spectrum of the product mixture for entry 9 reveals a resonance at 9.75 ppm ($\text{DMSO}-d_6$), signifying the presence of $(\text{DEAM-MBI})(\text{OTf})_2$ (**2-Me**).⁵⁷ Changing the catalyst loading, reaction temperature and pressure consistently produced **2-Me** (entries 9–11). These results indicate even a di-NHC ligand bound to Rh^I is susceptible to reductive elimination. Coupled with the Hg^0 poisoning experiments, this provides strong evidence the true identity of the active catalyst in entries 9–10 is Rh^0 .

To circumvent reductive elimination, one solution is to use a metal that provides stronger $\text{M}-\text{C}(\text{NHC})$ and $\text{M}-\text{H}$ bonds. Conveniently, iridium is a perfect candidate for a comparative study with **4-Me**. Using **3-ⁱPr** as the catalyst at 50 °C and 50 bar H_2 shows no conversion. However, no precipitate forms after 24 h, and the solution remains bright orange. A ^1H NMR spectrum of the solution reveals resonances attributed to **3-ⁱPr**, though the low catalyst loading precludes identification of all resonances. More importantly, the spectrum shows no signals corresponding to the imidazolium salt **2-ⁱPr**.

Since **3-ⁱPr** is not an effective catalyst for *trans*-methylstilbene hydrogenation, a rational next step is to use the activated substrate methyl-2-acetamidoacrylate. Table 4 summarizes methyl-2-acetamidoacrylate hydrogenation results. Performing the reaction at 50 °C and 50 bar H_2 in CDCl_3 with **4-Me** indicates full conversion occurs after 3 h, concomitant with formation of a black precipitate. These results, coupled with the observed 0% ee, prompted another Hg^0 experiment. As expected, adding Hg^0 prevents catalysis. However, when the size of the R-group on the catalyst is increased, decomposition products are not observed

Table 3 Metal catalyzed hydrogenation of *trans*-methylstilbene with **3** and **4**

Entry	Catalyst/loading (mol%)	Solvent	H_2 Pressure/bar	Temperature/°C	Mercury/g	Salt ^a	Conversion (%) ^b
1	4-Me (1)	CH_2Cl_2	50	40	0	N/A	>98
2	(<i>S</i>)- 4-Me (1)	CH_2Cl_2	50	40	0	N/A	>98
3	4-Me (1)	CH_2Cl_2	50	40	5.03	N/A	21
4	4-Me (1)	CH_2Cl_2	50	40	5.16	N/A	100
5	4-Me (1)	CH_2Cl_2	50	44	7.434	N/A	0
6	4-Me (10)	CDCl_3	50	40	7.011	Yes	0
7	$[\text{Rh}(\text{nbd})_2](\text{BF}_4)$ (1)	CH_2Cl_2	50	50	0	N/A	>98
8	$[\text{Rh}(\text{nbd})_2](\text{BF}_4)$ (1)	CH_2Cl_2	50	50	7.116	N/A	0
9	4-Me (10)	CDCl_3	50	50	0	Yes	80
10	4-Me (1)	CH_2Cl_2	50	25	0	Yes	>98
11	4-Me (1)	CH_2Cl_2	25	50	0	Yes	>98
12	3-ⁱPr (3)	CDCl_3	50	50	0	No	0
13	3-ⁱPr (5)	CDCl_3	100	97	0	Yes	>98

^a Presence of benzimidazolium salt by ^1H NMR. N/A means either NHC was not part of the catalyst or the salt was not looked for. ^b Determined by ^1H NMR spectroscopy after 24 h.

Table 4 Hydrogenation of methyl-2-acetamidoacrylate with **3** and **4**

Entry	Catalyst/loading (mol%)	Time/h	Hg	Conversion (%) ^a	ee (%) ^b
1	(<i>S</i>)- 4 -Me (1)	3	No	>98	0
2	(<i>S</i>)- 4 -Me (1)	24	Yes	0	N/A
3	(<i>S</i>)- 4 - ^{<i>i</i>} Pr (2)	24	No	100	8 (<i>R</i>)
4	(<i>S</i>)- 4 -diPh (2)	24	No	100	4 (<i>S</i>)
5	Ir(cod)acac (3)	3	No	>98	N/A
6	Ir(cod)acac (3)	24	Yes	0	N/A
7	(<i>S</i>)- 3 - ^{<i>i</i>} Pr (1.5)	24	No	>98	0
8	(<i>S</i>)- 3 - ^{<i>i</i>} Pr (1.5)	24	Yes	0	N/A
9	(<i>S</i>)- 3 -diPh (3)	36	No	93	9 (<i>R</i>)
10	(<i>S</i>)- 3 -diPh (3)	36	Yes	0	0

^a Determined by ¹H NMR (entries 1, 2, 5, 6) and GC-MS (entries 3, 4, 7–11). ^b Determined by GC-MS. Absolute configuration determined from literature precedent.

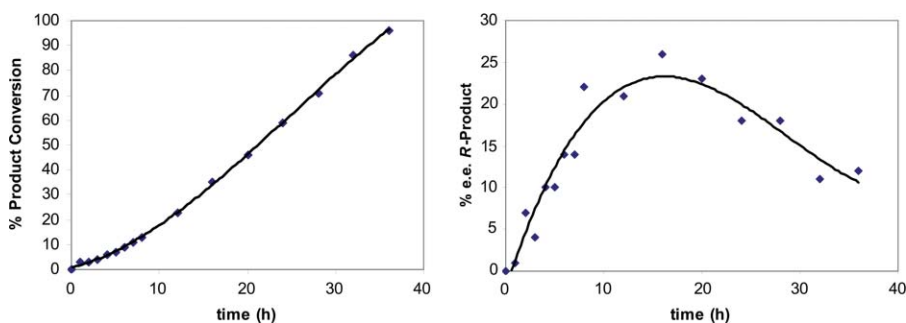


Fig. 4 Left: hydrogenation of methyl-2-acetamidoacrylate catalyzed by **3**-diPh (3 mol%); 50 bar H₂; 50 °C; CH₂Cl₂. Right: corresponding % ee vs. time curve.

in the ¹H NMR spectrum. In addition, GC analysis of the products show ee's of 8% (*R*) and 4% (*S*) for R = ^{*i*}Pr and diPh, respectively.

Changing to the Ir catalyst, **3**-^{*i*}Pr, shows complete hydrogenation after 24 h (entry 7). There is no detectable precipitate after the reaction and a bright orange solution remains. This suggests **3**-^{*i*}Pr survives, but a Hg⁰ poisoning experiment indicates no conversion after 24 h. Using **3**-diPh as the catalyst results in an ee of 9% favoring *R*-*N*-acetylalanine methyl ester with a conversion of 93% after 36 h. The Hg⁰ poisoning experiments show conversion is halted, suggesting Ir⁰ species, however achievement of enantioselectivity seems contradictory. As a control experiment, the iridium precursor was tested for hydrogenation, and is highly active. The mercury poisoning experiment demonstrated the expected sequestration.

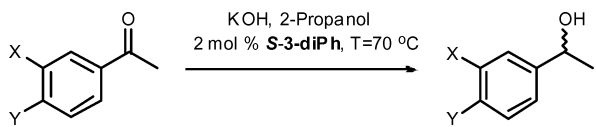
Fig. 4 (left) shows the kinetic profile for the hydrogenation of methyl-2-acetamidoacrylate with **3**-diPh as the catalyst. An induction period is observed followed by a linear profile. The linear portion implies zero-order kinetics in methyl-2-acetamidoacrylate. The induction period in the kinetic profile provides *prima facie* evidence for M⁰ species. MS analysis yielded a noteworthy peak at *m/z* 1099.3. The peak at 1099.3 contains an isotopic pattern indicative of [M]⁺ and is attributable to [**3**-diPh]⁺. Decomposition products, including the imidazolium salt **1**-diPh were not detected. A ¹H NMR spectrum of the product mixture did not reveal signals attributable to ligand loss. To amplify the

signal of possible decomposition products, **3**-diPh was subjected to catalytic conditions without the substrate. The ¹H NMR spectrum still reveals no signals attributed to decomposition products. This implies that only a small portion of **3**-diPh decomposes.

Fig. 4 (right) shows that the ee increases over time and then decreases, and is at a maximum at 16 h. Typically, an intact catalyst will start off at a given ee which will then decrease as the catalyst decomposes. A possible scenario that fits all of the data is an Ir⁰ species stabilized by the NHC ligand is the active catalyst, while the molecular species **3**-diPh is inactive.

It is reasonable to assume the reaction is first-order in catalyst. Doubling the loading of **3**-diPh doubles the yield, but halves the ee at *t* = 16 h. In a separate experiment, **3**-diPh (6 mol%) is pre-subjected to the reaction conditions without substrate to bypass the induction period and start with the active catalyst. After 24 h, the substrate is injected into the reactor and allowed to react for 16 h. The yield doubled and ee was again halved.

A few reported examples demonstrate an equilibrium between metal-bound NHC and free NHC can exist, as in the case of phosphine ligands.^{76–78} An excess of ligand was used to explore this unlikely equilibrium. In a catalytic hydrogenation reaction in which excess dibenzimidazolium salt and Cs₂CO₃ were added, the yield decreased to 5% and the ee was 6% (*S*). This result suggests the excess NHC ligand is actually serving to poison the catalyst, as previously demonstrated by Finke *et al.*⁷⁹

Table 5 Hydrogen transfer of methyl ketones with **3-diPh**


Entry	Time/h	X	Y	Conversion (%) ^a	ee (%) ^b
1	1	H	H	18	5 (<i>R</i>)
2	5	H	H	>98	6 (<i>R</i>)
3	5	C ₄ H ₄	H	>98	3 (<i>R</i>)
4	5	H	Br	>98	5 (<i>R</i>)
5	5	Br	H	>98	5 (<i>R</i>)

^a Determined by ¹H NMR. ^b Determined by HPLC. Absolute configuration determined from literature precedent.

In summary, there is strong evidence to implicate M⁰ species as the active catalyst, however there does not appear to be a way to maximize both % conversion and ee.

Hydrogenation of methyl ketones

3-diPh was evaluated as a catalyst for hydrogen transfer reactions of methyl ketones. Table 5 summarizes the results. The reaction was carried out at 70 °C for 5 h in 2-propanol at 2 mol% catalyst loading with KOH as the base. The conversion is complete after 5 h, but the % ee is low and favoring the *R* enantiomer in each case. The solution at the beginning of the reaction is bright orange and then turns dark orange by the end. Visual inspection of the solution at the end of the reaction does not show a precipitate, and the ¹H NMR did not show any resonances connected to ligand loss. Typically, high temperatures have an adverse effect on ee, and as time progresses ee decreases. The ee was checked after an hour during the hydrogenation of acetophenone, demonstrating no change between *t* = 1 and *t* = 5 h (entries 1 and 2). Lowering the temperature to 50 °C reduces the conversion to zero after 24 h. Remember that **5-Me** displays a degenerate isomerization, with the

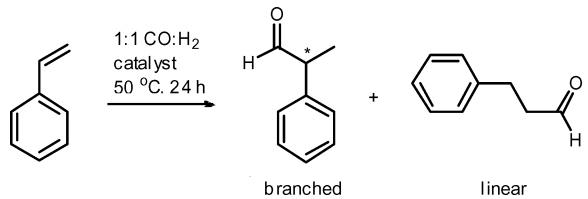
exchange rate increasing with temperature. The first step during the catalytic cycle is most likely loss of cod from **3-diPh**. Therefore, a likely explanation for the low ee in the hydrogenation reactions could be an ill-defined chiral pocket caused by the floppy nature of the ligand.

Hydroformylation of styrene

Catalysts bearing NHC ligands are less established in hydroformylation reactions than in palladium catalyzed coupling reactions or ruthenium olefin metathesis reactions.⁸⁰ Of these reactions, few catalysts make use of di-NHC ligands, and surprisingly there are no reports of enantioselective hydroformylation. The rhodium catalysts **4-R**, **5-Me** and **6-Me** were screened for the hydroformylation of styrene. **6-Me** is a bimetallic complex ([μ-(DEAM-RBY)][Rh(COD)Cl]₂) synthesized from [Rh(cod)Cl]₂ which was previously reported.⁵⁷ Table 6 shows the results.

Generally, product formation is complete after 24 h at 50 °C with catalyst loadings of 0.1 mol%. Solvent effects appear to have little effect on either conversion or branched to linear ratios. Pressures of less than 80 bar reduced the conversion to zero. The branched to linear ratios (b:l) are all suspiciously similar, approximately 96:4. In a study of common hydroformylation precatalysts, the b:l ratios ranged from 95:5 to 98:2, implying a common catalyst.⁸¹ This prompted an investigation into the catalyst identity.

There were no black precipitates at the end of the reaction to signal decomposition occurred. A mercury poisoning experiment inhibited catalysis. Since the hydroformylation products are volatile, decomposition products were easily isolated. A ¹H NMR spectrum clearly shows all the resonances associated with the Me-dibenzimidazolium salt. Furthermore, the control experiment using [Rh(nbd)₂](BF₄) as the hydroformylation catalyst showed a b:l of 98:2. Following the hydroformylation kinetics of styrene with **5-Me** demonstrated a sigmoidal curve (Fig. 5). In summary, the b:l ratio indicates a common species is responsible for hydroformylation. Considering the common b:l and an observed induction period (Fig. 5), the most likely species is Rh(CO)₄H.⁸⁰⁻⁸²

Table 6 Hydroformylation of styrene with **4-R**, **5-Me** and **6-R**


Entry	Catalyst/loading (mol%)	Pressure/bar	Solvent	Conversion (%) ^a	Branched : linear ^a
1	(<i>S</i>)- 4-Me (1)	50	Chloroform	0	N/A
2	(<i>S</i>)- 4-Me (1)	100	Chloroform	100	95 : 5
3	(<i>S</i>)- 4-Me (0.1)	100	Chloroform	100	96 : 4
4	(<i>S</i>)- 4-diPh (5)	100	Toluene	96	96 : 4
5	(<i>S</i>)- 5-Me (0.1)	30	Chloroform	0	N/A
6	(<i>S</i>)- 5-Me (0.1)	50	Chloroform	0	N/A
7	(<i>S</i>)- 5-Me (0.1)	80	Chloroform	100	97 : 3
8	(<i>S</i>)- 5-Me (0.1)	80	Toluene	100	96 : 4
9	(<i>S</i>)- 6-Me (0.1)	100	Chloroform	75	94 : 6
10	(<i>S</i>)- 6-Me (0.1)	100	Toluene	100	94 : 6
11	[Rh(nbd) ₂](BF ₄) (0.1)	100	Chloroform	100	97 : 3

^a Determined by GC.

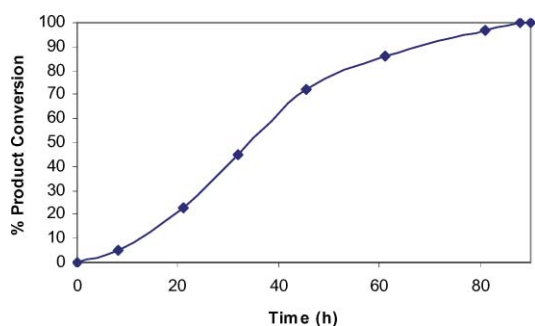


Fig. 5 Hydroformylation of styrene catalyzed by **5-Me** (0.01 mol%): 80 bar syngas; 50 °C; CHCl_3 .

$\text{Rh}(\text{CO})_4\text{H}$ is difficult to observe due to the stability of the complex outside hydroformylation conditions. Recently, Garland *et al.* successfully found this species by IR spectroscopic means during the hydroformylation of alkenes with the metal precursor, $\text{Rh}_4(\text{CO})_{12}$.⁸²

Conclusions

In summary, we report the synthesis of new iridium and rhodium complexes supported by a chiral ethanoanthracene ligand bearing two NHC moieties (DEAM-RBY). The complexes **3-ⁱPr** and **5-Me** form single crystals and permit X-ray structural analysis. Complex **5-Me** undergoes a degenerate isomerism in the solution state and multinuclear NMR spectroscopic techniques indicate the barrier to ring inversion is $16.9 \pm 1.8 \text{ kcal mol}^{-1}$ with an associated entropy of activation that is small and negative ($-7 \pm 6 \text{ cal mol}^{-1} \text{ K}^{-1}$).

Under hydrogenation conditions the catalysts decompose into the corresponding M^0 species, presumably *via* $[\text{NHC-H}]^+$ reductive elimination. Mercury poisoning experiments prevent catalytic turnover and supports M^0 as the active catalyst. In addition, kinetic studies reveal an induction period, indicative of M^0 formation. Monitoring the ee with respect to time provides further evidence for the growth of M^0 particles. As the reaction proceeds the ee changes from 0% to a maximum of 25%, followed by a decrease to the final ee of 9%. In the examples that show enantioselectivity, the ligand must be associated with the metal particle during catalysis. Only a few documented examples exist for enantioselective catalysis by a M^0 species.^{83–85} For example, nano-sized M^0 species are implicated in the hydrogenation of ethyl pyruvate using Pt and Pd precatalysts. Thus, one explanation for the change in ee is the M^0 particle size must change with time. As the particle grows, the influence of the ligand on selectivity will change as function of surface area. A maximum is reached once the optimum surface area/ligand coverage is achieved for the system, but as more M^0 species are initiated the selectivity drops.

The hydroformylation experiments also indicate reductive elimination is a facile process for catalysts supported by di-NHCs. The similar b:l ratios indicate a common catalyst is most likely operating. It is well documented that $\text{RhH}(\text{CO})_4$ can form under hydroformylation conditions from a variety of Rh precursors. Under a CO atmosphere, if the NHC reductively eliminates, Rh⁰ deposition is prevented and $\text{RhH}(\text{CO})_4$ forms.

Though the evidence strongly supports ligand reductive elimination, it is plausible that the low ee is due to the flexible nature of

the ligand, whether on the surface of a particle or as a molecular species. Only a 16 kcal mol⁻¹ barrier is associated with the ring inversion in **5-Me**. Perhaps this flexibility presents too many degrees of freedom for the incoming substrate and chirality defining step during catalysis. Forthcoming next generation ligands will impart a more rigid and defined chiral pocket.

Experimental

General methods

Unless specified otherwise, all manipulations were performed under an inert atmosphere using standard Schlenk or glovebox techniques. Glassware was oven dried before use. Tetrahydrofuran (THF), 1,2 dimethoxyethane (DME) and dichloromethane (CH_2Cl_2) were dried using a GlassContours drying column. C_6D_6 (Cambridge Isotopes) was dried over sodium–benzophenone ketyl, distilled, vacuum transferred and stored over 4 Å molecular sieves. CDCl_3 (Cambridge Isotopes) was dried over calcium hydride, distilled, vacuum transferred and stored over 4 Å molecular sieves. (1,5-Cyclooctadiene)iridium(I)(acetylacetonate), (cod)Ir(acac), and bis-norbornadiene-rhodium(I) tetrafluoroborate, $[\text{Rh}(\text{nbd})](\text{BF}_4)$, were purchased from Strem Chemicals Inc. and used without further purification. Cesium carbonate (Cs_2CO_3), *trans*-methylstilbene, methyl-2-acetamidocrylate, acetophenone, 1-(2-naphthalenyl)ethanone, 1-(4-bromophenyl)ethanone, 1-(3-bromophenyl)ethanone, benzimidazole, potassium bis-trimethylsilylamide $\text{KN}(\text{Si}(\text{CH}_3)_3)_2$ and chlorodiphenylmethane were purchased from Sigma-Aldrich and used without further purification. Anhydrous potassium carbonate (K_2CO_3), styrene, anhydrous sodium sulfate (Na_2SO_4), potassium hydroxide (KOH), Celite, xylenes, ether, 2-propanol and hexanes were purchased from Fisher Scientific and used without further purification. Syngas, carbon monoxide and hydrogen were purchased from Airgas. The synthetic procedure for **2-ⁱPr** was reported previously.⁵⁷ NMR spectra were obtained on Varian Mercury Broad Band 300 MHz, Varian Mercury 300 MHz, or INOVA 500 MHz spectrometers. Chemical shifts are reported in δ (ppm). For ^1H and $^{13}\text{C}\{^1\text{H}\}$ NMR spectra, the residual proton solvent peak was referenced as an internal reference. IR spectra were recorded on a Thermo Nicolet Nexus 670-FT-IR spectrometer. Spectra of solids were measured as KBr discs. Mass spectrometry was performed at the in-house facility of the Department of Chemistry at the University of Florida. Chemical ionization, electrospray ionization, and MALDI-TOF methods were used. Combustion analyses were performed by E and R MicroAnalytical Division, Parsippany, NJ or at the in-house facility of the Department of Chemistry at the University of Florida. For HPLC analysis, a Shimadzu prominence system with a LC-20AT solvent delivery module, DGU-20A3 degasser, SPD-20A UV-vis detector (225 or 254 nm), and a CBM-20A system controller were used. GC and GC-MS analyses were carried out on a Thermo-Scientific Trace DSQ mass spectrometer.

Synthesis of 1-diphenylmethanebenzimidazole (**1**)

To a 1 L round bottom flask was added the following reagents in the order listed: benzimidazole (12.00 g, 0.102 mol), 500 mL xylenes, anhydrous K_2CO_3 (14.16 g, 0.102 mol), KOH

(6.01 g, 0.107 mol) and tetra(*n*-butyl)ammonium bromide (1.70 g, 5.27 mmol). The flask was then attached to a condenser with argon flowing through it. The contents of the flask were stirred for 5 min at room temperature and then chlorodiphenylmethane (18.0 mL, 0.124 mmol) was added through the top of the condenser. The reaction was heated at reflux under argon. After 26 h, the reaction mixture was filtered hot through Celite. The filtrate was dried over anhydrous Na₂SO₄, filtered and all volatiles removed *in vacuo* to provide a beige oil. A solution of 3:2 ethyl acetate:hexanes (300 mL) was added to the oil inducing precipitation. The solution was stirred with a glass rod for 20 min and then the precipitate was filtered through a coarse fritted funnel. The precipitate was then washed with ether (3 × 15 mL) providing **1** as a white powder (18.20 g, 63%). Found: C, 84.45%; H, 5.81%; N, 9.51%. calc. for C₂₀H₁₆N₂: C, 84.46%; H, 5.68%; N, 9.85%. ¹H NMR (300 MHz, CDCl₃, δ): 8.31 (d, *J* = 9 Hz, 1H, NCHN), 8.05 (d, *J* = 9 Hz, 1H, NCHNCCH), 7.58/7.55 (d, *J* = 9 Hz, 1H, NCCHCH), 7.51–7.41 (m, 6H, C₆H₃), 7.32 (d, *J* = 9 Hz, 1H, CHNCCH), 7.22–7.15 (m, 4H, C₆H₃), 6.97 (d, *J* = 9 Hz, 1H, CCHNC). ¹³C NMR (75.36 MHz, (CD₃)₂SO, δ): 143.6 (CHNCHNC), 142.8 (NCHN), 138.7 (NCHC), 133.9 (CHNC), 128.8 (NCHCCHCH), 128.1 (NCHCCHCHCH), 128.0 (NCHCCH), 122.5 (CHNCCHCH), 121.8 (NCHNCCHCH), 119.7 (NCHNCCH), 111.2 (CHNCCH), 61.9 (NCHC).

Synthesis of *trans*-9,10-dihydro-9,10-ethanoanthracene-11,12-bis(1-diphenylmethane)-benzimidazolium (DEAM-diPh)(OTf) (2-diPh)

To a 100 mL flask containing 9,10-dihydro-9,10-ethanoanthracene-11,12-diyl dimethanediyl bis(trifluoromethanesulfonate) (2.01 g, 3.79 mmol) dissolved in anhydrous DME (50 mL) was added **1** (2.26 g, 7.95 mmol). After refluxing under argon for 75 min, the solution was reduced *in vacuo* to approximately 15 mL. A precipitate formed and was filtered through a coarse fritted funnel. The precipitate was washed with ether (4 × 15 mL) providing **2-diPh** as a mildly hygroscopic white powder (3.13 g, 75%). Found: C, 64.66%; H, 4.80%; N, 4.62%. Calc. for (C₃₈H₄₈N₄(O₃SCF₃)₂ + 1 molecule DME (C₄H₁₀O₂) C, 64.62%; H, 4.93%; N, 4.71%. ¹H NMR (300 MHz, (CD₃)₂SO, δ): 9.29 (s, 2H, NCHN), 7.97 (dd, *J* = 3 Hz, *J* = 3 Hz, 2H, NCCH), 7.85 (dd, *J* = 3 Hz, *J* = 3 Hz, 2H, NCCH), 7.74 (dd, *J* = 3 Hz, *J* = 3 Hz, 4H, CC₅H₅-aromatic), 7.65 (s, 2H, NCH), 7.62–7.43 (m, 20H, aromatic), 7.27 (d, *J* = 6 Hz, 2H, CH₂CHCHCCHCH), 7.17 (dd, *J* = 9 Hz, *J* = 9 Hz, 2H, NCCHCH), 7.02 (dd, *J* = 9 Hz, *J* = 9 Hz, 2H, NCCHCH), 6.84 (d, *J* = 6 Hz, 2H, CH₂CHCHCCH), 4.52 (dd, *J* = 15 Hz, *J* = 3 Hz, 2H, CHH), 4.12 (s, 2H, CH₂CHCH), 3.93 (dd, *J* = 15 Hz, *J* = 9 Hz, 2H, CHH), 3.43 (s, DME), 3.24 (s, DME), 2.41 (m, 2H, CH₂CHCH). ¹³C NMR (75.36 MHz, (CD₃)₂SO, δ): 142.6 (s, NCN), 142.0 (CCHC), 139.2 (CCHC), 135.9 (NCHC), 135.9 (NCHC), 131.6 (NCCH), 131.4 (NCCH), 129.3 (CC₅H₅), 129.2 (CC₅H₅), 129.1 (CC₅H₅), 129.0 (CC₅H₅), 128.1 (CC₅H₅), 127.1 (NCCHCH), 127.1 (NCCHCH), 126.4 (CH₂CHCHCCH), 126.1 (CH₂CHCHCCH), 125.2 (CH₂CHCHCCHCH), 124.0 (CH₂CHCHCCHCH), 120.7 (q, *J* = 323 Hz, CF₃), 114.6 (NCCH), 114.0 (NCCH), 71.0 (DME), 64.3 (NCH), 58.0 (DME), 50.1 (NCH₂), 43.9 (CCHCHCH₂), 42.2 (NCH₂CH).

Synthesis of iridium(i) *trans*-9,10-dihydro-9,10-ethanoanthracene-11,12-bis(1-diphenylmethane-benzimidazolide-2-ylidene) 1,5-cyclooctadiene triflate, [(DEAM-diPh)Ir(cod)](OTf) (3-diPh)

To a THF solution (2 mL) of **2-diPh** (432 mg, 0.393 mmol) and Cs₂CO₃ (269 mg, 0.823 mmol) was added a solution of (cod)Ir(acac) (157 mg, 0.393 mmol in 2 mL THF) at 23 °C. After stirring the solution overnight it was filtered and the filtrate dropped into 20 mL of hexanes to form a precipitate. The precipitate was filtered and dried on a high vacuum line providing **3-diPh** as a bright orange powder (422 mg, 89%). Found: C, 65.24%; H, 4.59%; N, 4.40%. Calc. for IrC₆₇H₅₈N₄SO₃F₃: C, 64.45%; H, 4.69%; N, 4.48%. ¹H NMR (500 MHz, CDCl₃, δ): 8.38 (s, 1H, NCH), 8.04 (d, *J* = 10 Hz, 1H, NCCH), 7.74 (d, *J* = 5 Hz, 1H, aromatic), 7.57 (d, *J* = 5 Hz, 1H, aromatic), 7.49–7.04 (m, 20H, aromatic), 6.96 (s, 1H, NCH), 6.90 (dd, *J* = 5 Hz, *J* = 5 Hz, 1H, aromatic), 6.86–6.76 (m, 6H, aromatic), 6.62 (d, *J* = 5 Hz, 1H, NCCH), 6.55 (d, *J* = 5 Hz, 2H, aromatic), 6.36 (d, *J* = 10 Hz, 1H, NCCH), 6.14 (d, *J* = 5 Hz, 2H, aromatic), 5.32 (d, *J* = 15 Hz, 1H, NCHH), 4.98 (s, 1H, NCH₂CHCH), 4.73–4.68 (m, 2H, IrCH, NCHH), 4.40 (s, 1H, NCH₂CHCH), 4.30–4.18 (m, 2H, NCHH, NCH₂CH), 3.68–3.55 (m, 2H, IrCH), 2.90 (d, *J* = 9 Hz, 1H, NCHH), 2.78 (d, *J* = 5 Hz, 1H, IrCH), 2.14–2.05 (br. s, 1H, NCH₂CH), 2.02–1.85 (m, 2H, IrCHCH₂), 1.67–1.53 (m, 3H, IrCHCH₂), 1.30–1.16 (m, 2H, IrCHCH₂), 0.57–0.44 (m, 1H, IrCHCH₂). ¹³C NMR (75.36 MHz, CDCl₃, δ): 189.9 (IrCN), 187.0 (IrCN), 145.5 (CCHC), 144.0 (CCHC), 139.1 (CCHC), 138.3 (CCHC), 137.8 (NCHC), 137.0 (NCHC), 136.8 (NCHC), 135.9 (NCHC), 135.8 (NCCH), 135.4 (NCCH), 133.9 (NCCH), 133.2 (NCCH), 129.2 (C aromatic), 128.9 (C aromatic), 128.7 (C aromatic), 128.6 (C aromatic), 128.4 (C aromatic), 127.9 (C aromatic), 127.6 (C aromatic), 127.0 (C aromatic), 126.9 (C aromatic), 126.8 (C aromatic), 126.6 (C aromatic), 126.3 (C aromatic), 125.3 (C aromatic), 124.4 (C aromatic), 124.3 (C aromatic), 123.8 (C aromatic), 123.8 (C aromatic), 123.6 (C aromatic), 122.9 (C aromatic), 115.2 (s, NCCH), 113.6 (s, NCCH), 111.8 (NCCH), 110.0 (NCCH), 85.8 (IrCH), 81.4 (IrCH), 75.1 (IrCH), 72.4 (IrCH), 68.9 (NCH), 68.2 (NCH), 54.7 (NCH₂), 51.5 (NCH₂), 51.2 (NCH₂CH), 46.9 (NCH₂CHCH), 46.8 (NCH₂CHCH), 45.9 (NCH₂CH), 36.8 (IrCHCH₂), 35.5 (IrCHCH₂), 25.8 (2 overlapping IrCHCH₂).

Synthesis of iridium(i) *trans*-9,10-dihydro-9,10-ethanoanthracene-11,12-bis(1-isopropylbenzimidazolide-2-ylidene) 1,5-cyclooctadiene triflate, [(DEAM-IBY)Ir(cod)](OTf) (3-ⁱPr)

To a THF solution (2 mL) of **2-ⁱPr** (428 mg, 0.503 mmol) and Cs₂CO₃ (340 mg, 1.04 mmol) was added a solution of (cod)Ir(acac) (198 mg, 0.496 mmol in 2 mL THF) at 23 °C. After stirring the solution overnight it was filtered. The filtrate was then dropped into 20 mL of hexanes to form a precipitate. The precipitate was filtered and dried on a high vacuum line providing **3-ⁱPr** as a bright orange powder (490 mg, 99%). Found: C, 56.21%; H, 5.08%; N, 5.25%. Calc. for IrC₄₇H₅₀N₄SO₃F₃: C, 56.43%; H, 5.05%; N, 5.60%. ¹H NMR (300 MHz, CDCl₃, δ): 7.90 (d, *J* = 9 Hz, 1H, aromatic), 7.73 (dd, *J* = 3 Hz, *J* = 6 Hz, 1H, aromatic), 7.67 (dd, *J* = 3 Hz, *J* = 6 Hz, 1H, aromatic), 7.53 (dd, *J* = 3 Hz, *J* = 6 Hz, 1H, aromatic), 7.43–7.16 (m, 12 H, aromatic), 6.23 (septet, *J* = 6 Hz, 1H, CH(CH₃)₂), 5.13 (d, *J* = 12 Hz, 1H, NCHH), 5.05 (septet,

$J = 6$ Hz, 1H, $\text{CH}(\text{CH}_3)_2$), 4.83 (d, $J = 3$ Hz, 1H, CCHC), 4.67–4.55 (m, 3H, overlapping signals; NCHH, IrCH, IrCH), 4.17 (d, $J = 3$ Hz, 1H, CCHC), 3.99 (ddd, $J = 6$ Hz, $J = 6$ Hz, $J = 1$ Hz, 1H, NCH_2CH), 3.80 (dd, $J = 12$ Hz, $J = 12$ Hz, 1H, NCHH), 3.62 (dt, $J = 6$ Hz, $J = 6$ Hz, 1H, IrCH), 2.74 (dt, $J = 6$ Hz, $J = 6$ Hz, 1H, IrCH), 2.57–2.44 (m, 1H, IrCHCHH), 2.36 (ddd, $J = 6$ Hz, $J = 6$ Hz, $J = 1$ Hz, 1H, NCH_2CH), 2.28 (d, $J = 15$ Hz, 1H, NCHH), 2.19–2.08 (m, 1H, IrCHCHH) 2.02 (d, $J = 6$ Hz, 3H, $\text{CH}(\text{CH}_3)_2$), 1.80 (d, $J = 6$ Hz, 3H, $\text{CH}(\text{CH}_3)_2$), 1.66 (d, $J = 6$ Hz, 3H, $\text{CH}(\text{CH}_3)_2$), 1.88–1.58 (m, 4H, signals overlap with isopropyl methyls, IrCHCHH), 1.46–1.35 (m, 1H, IrCHCHH), 0.91 (d, $J = 6$ Hz, 3H, $\text{CH}(\text{CH}_3)_2$), 0.65–0.51 (m, 1H, IrCHCHH). ^{13}C NMR (75.36 MHz, CDCl_3 , δ): 188.1 (NCN), 183.8 (NCN), 145.2 (CCHC), 143.7 (CCHC), 139.0 (CCHC), 138.4 (CCHC), 136.2 (NCCH), 135.8 (NCCH), 132.1 (NCCH), 131.4 (NCCH), 127.0 (CCHCHCH), 126.9 (CCHCHCH), 126.7 (CCHCHCH), 126.4 (CCHCHCH), 126.2 (CCHCCH), 125.2 (CCHCCH), 124.2 (CCHCCH), 124.1 (NCCHCH), 123.8 (NCCHCH), 123.8 (NCCHCH), 123.6 (NCCHCH), 122.9 (CCHCCH), 121.0 (q, $J = 321$ Hz, CF_3), 113.2 (NCCH), 112.5 (NCCH), 111.7 (NCCH), 110.2 (NCCH), 85.6 (IrCH), 79.1 (IrCH), 75.3 (IrCH), 69.2 (IrCH), 55.7 ($\text{CH}(\text{CH}_3)_2$), 54.8 ($\text{CH}(\text{CH}_3)_2$), 54.7 (NCH_2), 51.7 (NCH_2), 50.8 (NCH_2CH), 47.2 (CCHC), 47.0 (CCHC), 46.0 (NCH_2CH), 37.1 (IrCHCH $_2$), 35.7 (IrCHCH $_2$), 28.0 (IrCHCH $_2$), 26.2 (IrCHCH $_2$), 22.6 ($\text{CH}(\text{CH}_3)_2$), 21.2 ($\text{CH}(\text{CH}_3)_2$), 21.0 ($\text{CH}(\text{CH}_3)_2$), 20.9 ($\text{CH}(\text{CH}_3)_2$). MS(HR-ESI-FTICR+): Calc. for $[\text{C}_{46}\text{H}_{50}\text{N}_4\text{Ir}]^+$: m/z 849.3636 M^+ , Found m/z 849.3572.

Synthesis of rhodium(I) *trans*-9,10-dihydro-9,10-ethanoanthracene-11,12-bis(1-diphenylmethane-benzimidazolidine-2-ylidene)norbornadiene triflate, [(DEAM-diPhBY)Rh(nbd)](OTf) (4-diPh)

To a THF (2 mL) solution of 2-diPh (294 mg, 0.268 mmol) was slowly added a solution of $\text{KN}(\text{Si}(\text{CH}_3)_3)_2$ (112 mg, 0.563 mmol) in 3 mL THF at -35 °C in a glovebox. After stirring this solution for 10 min at room temperature, it was cooled to -35 °C. To this solution was then added a solution of $[\text{Rh}(\text{nbd})_2](\text{BF}_4)$ (101 mg, 0.270 mmol in 4 mL) and the final solution was kept at -35 °C overnight. On the bench top the solution was filtered through a 0.2 μm nylon filter into a stirring solution of hexanes. After 10 min the yellow precipitate that forms was collected on a fine fritted funnel and washed with ether (3 \times 15 mL). The precipitate was dried providing 4-diPh as a golden yellow powder (269 mg, 88%). Found: C, 68.77%; H, 4.98%; N, 4.64%. Calc. for $\text{RhC}_{66}\text{H}_{54}\text{N}_4\text{SO}_3\text{F}_3$: C, 69.35%; H, 4.76%; N, 4.90. ^1H NMR (300 MHz, CDCl_3 , δ): 8.53 (s, 1H, NCH), 8.02 (d, $J = 6$ Hz, 1H, NCCH), 7.86 (d, $J = 6$ Hz, 1H, aromatic), 7.59 (d, $J = 9$ Hz, 1H, aromatic), 7.45–6.75 (m, 30H, aromatic), 7.24 (s, 1H, NCH), 6.62 (d, $J = 9$ Hz, 1H, NCCH), 6.22 (d, $J = 9$ Hz, 2H, NCCH and aromatic), 5.37 (d, $J = 12$ Hz, 1H, NCHH), 5.17 (dd, $J = 9$ Hz, $J = 9$ Hz, 1H, NCH_2CH), 5.00 (s, 1H, NCH_2CHCH), 4.80–4.72 (m, 2H, RhCH and NCHH), 4.42 (br s, 1H, RhCH), 4.35 (s, 1H, NCH_2CHCH), 4.21 (dd, $J = 15$, $J = 12$, 1H, NCHH) 3.88 (br s, 1H, RhCH), 3.46 (br s, 1H, RhCHCH), 3.33 (br s, 1H, RhCH), 3.03–2.99 (m, 2H, NCHH, RhCHCH), 2.18 (dd, $J = 9$ Hz, $J = 9$ Hz, 1H, NCH_2CH), 1.23 (dd, $J = 9$ Hz, $J = 9$ Hz, 1H, RhCHCHCHH), 1.19 (dd, $J = 9$ Hz, $J = 9$ Hz, 1H, RhCHCHCHH). ^{13}C NMR (75.36 MHz, CDCl_3 , δ): 194.9 (d, $J = 57$, RhCN), 194.7 (d, $J = 57$, RhCN), 144.8

(CCHC), 144.0 (CCHC), 139.2 (CCHC), 138.3 (CCHC), 137.7 (NCHC), 137.6 (NCHC), 137.0 (NCHC), 136.2 (NCHC), 135.9 (2 overlapping signals, NCCH), 133.7 (NCCH), 133.1 (NCCH), 129.4 (C aromatic), 129.0 (C aromatic), 128.8 (C aromatic), 128.7 (C aromatic), 128.6 (C aromatic), 128.5 (C aromatic), 128.4 (C aromatic), 128.3 (C aromatic), 127.8 (C aromatic), 127.7 (C aromatic), 127.3 (C aromatic), 127.2 (C aromatic), 126.9 (C aromatic), 126.8 (C aromatic), 126.7 (C aromatic), 126.6 (C aromatic), 126.3 (C aromatic), 125.3 (C aromatic), 124.5 (q, $J = 321$, CF_3), 124.1 (C aromatic), 124.0 (C aromatic), 123.9 (C aromatic), 123.5 (C aromatic), 123.3 (C aromatic), 122.8 (C aromatic), 114.4 (NCCH), 113.0 (NCCH), 111.4 (NCCH), 109.9 (NCCH), 80.9 (d, $J = 7.5$, RhCH), 75.4 (d, $J = 7.5$, RhCH), 70.7 (d, $J = 7.5$, RhCH), 68.8 (NCH), 68.6 (NCH), 68.05 (RhCHCHCH $_2$), 67.3 (d, $J = 7.5$, RhCH), 54.6 (NCH_2), 52.5 (RhCHCH), 52.3 (NCH_2CH), 51.5 (RhCHCH), 50.5 (NCH_2), 46.9 (NCH_2CHCH), 46.7 (NCH_2CHCH), 45.2 (NCH_2CH). MS(HR-ESI-FTICR+): Calc. for $[\text{C}_{65}\text{H}_{54}\text{N}_4\text{Rh}]^+$: m/z 993.3398 M^+ , Found m/z 993.3399.

Synthesis of rhodium(I) *trans*-9,10-dihydro-9,10-ethanoanthracene-11,12-bis(1-isopropylbenzimidazolidine-2-ylidene)norbornadiene triflate, [(DEAM-IBY)Rh(nbd)](OTf) (4- i Pr)

To a THF (2 mL) solution of 2- i Pr (108 mg, 0.127 mmol) was slowly added a solution of $\text{KN}(\text{Si}(\text{CH}_3)_3)_2$ (56 mg, 0.281 mmol) in 3 mL THF at -35 °C in a glovebox. After stirring this solution for 10 min at room temperature, it was cooled to -35 °C. To this solution was then added a solution of $[\text{Rh}(\text{nbd})_2](\text{BF}_4)$ (54 mg, 0.144 mmol in 4 mL) and the final solution was kept at -35 °C overnight. On the bench top the solution was filtered through a 0.2 μm nylon filter into a stirring solution of hexanes. After 10 min the yellow precipitate that forms was collected on a fine fritted funnel and washed with ether (3 \times 15 mL). The precipitate was dried providing 4- i Pr as a golden yellow powder (110 mg, 92%). Found: C, 61.71%; H, 5.20%; N, 6.23%. Calc. for $\text{RhC}_{46}\text{H}_{46}\text{N}_4\text{SO}_3\text{F}_3$: C, 61.73%; H, 5.19%; N, 6.26. ^1H NMR (300 MHz, CDCl_3 , δ): 7.77 (dd, $J = 9$ Hz, $J = 9$ Hz, 2H, aromatic), 7.66 (dd, $J = 3$ Hz, $J = 6$ Hz, 2H, aromatic), 7.55 (dd, $J = 3$ Hz, $J = 6$ Hz, 2H, aromatic), 7.38–7.14 (m, 10 H, aromatic), 6.38 (septet, $J = 6$ Hz, 1H, $\text{CH}(\text{CH}_3)_2$), 5.34 (septet, $J = 6$ Hz, 1H, $\text{CH}(\text{CH}_3)_2$), 5.22 (dd, $J = 6$ Hz, $J = 9$ Hz, 1H, NCH_2CH), 5.09 (d, $J = 12$ Hz, 1H, NCH_2), 4.82 (s, 1H, NCH_2CHCH), 4.71–4.62 (m, 4H, RhCH (3H) and NCH_2), 4.19 (s, 1H, NCH_2CHCH), 4.10 (br s, 1H, RhCHCH), 3.81 (m, 1H, RhCH), 3.70 (dd, $J = 9$ Hz, $J = 12$ Hz, 1H, NCH_2), 2.96 (br s, 1H, RhCHCH), 2.34 (s, 1H, NCH_2), 2.03 (br s, 1H, NCH_2CH), 1.94 (d, $J = 6$ Hz, 3H, $\text{CH}(\text{CH}_3)_2$), 1.86 (d, $J = 6$ Hz, 3H, $\text{CH}(\text{CH}_3)_2$), 1.60 (d, $J = 6$ Hz, 3H, $\text{CH}(\text{CH}_3)_2$), 1.41 (dd, $J = 9$ Hz, $J = 9$ Hz, 1H, RhCHCHCHH), 1.39 (dd, $J = 9$ Hz, $J = 9$ Hz, 1H, RhCHCHCHH), 1.04 (d, $J = 6$ Hz, 3H, $\text{CH}(\text{CH}_3)_2$). ^{13}C NMR (75.36 MHz, CDCl_3 , δ): 192.1 (d, RhCN, $J = 57$), 191.9 (d, RhCN, $J = 57$), 144.6 (CCHC), 143.9 (CCHC), 139.1 (CCHC), 138.5 (CCHC), 136.5 (NCCH), 136.3 (NCCH), 132.0 (NCCH), 131.3 (NCCH), 129.0 (CHCCHCH), 128.2 (CHCCHCH), 126.9 (CHCCHCH), 126.5 (CHCCHCH), 126.4 (NCCHCH), 125.3 (NCCHCH), 124.0 (NCCHCH), 123.6 (CHCCH), 123.5 (CHCCH), 123.3 (CHCCH), 123.1 (CHCCH), 122.9 (NCCHCH), 112.9 (NCCH), 112.0 (NCCH), 111.0 (NCCH), 109.7 (NCCH), 80.3 (d, RhCH, $J = 7.5$), 74.5 (d, RhCH, $J = 7.5$), 70.6 (d, RhCH, $J = 7.5$), 67.8 (RhCHCHCH $_2$),

65.1 (d, RhCH, $J = 7.5$), 55.8 (CHCH₃), 55.2 (CHCH₃), 54.5 (NCH₂), 52.4 (RhCHCH), 52.0 (RhCHCH), 51.7 (NCH₂CH), 49.8 (NCH₂), 47.2 (NCH₂CHCH), 46.6 (NCH₂CHCH), 45.2 (NCH₂CH), 22.5 (CHCH₃), 21.5 (CHCH₃), 21.3 (CHCH₃), 21.1 (CHCH₃). MS(HR-ESI-FTICR+): Calc. for [C₄₅H₄₆N₄Rh]⁺: m/z 745.2772 M⁺, Found m/z 745.2782.

Synthesis of the rhodium(I) *trans*-9,10-dihydro-9,10-ethanoanthracene-11,12-bis(1-methylbenzimidazolide-2-ylidene)bis-carbon monoxide tetrafluoroborate, [(DEAM-MbBI)Rh(CO)₂](BF₄) (5-Me)

To a Parr Instruments 45 mL capacity autoclave was added a stir bar, [(DEAM-MBY)Rh(nbd)](OTf) (600 mg, 0.716 mmol) and 12 mL chloroform. The autoclave was then charged with 100 bar of carbon monoxide and stirred at 50 °C for 24 h. The autoclave was then discharged, and the chloroform was washed with deionized water (3 × 10 mL). The chloroform was removed *in vacuo* to provide 5-Me as a yellow powder (584 mg, 92%). IR (KBr, cm⁻¹): 2025.8 s (CO), 2083.6 s (CO). Found C, 47.08%; H, 3.26%; N, 6.10%. Calc. for RhC₃₈H₃₂N₄O₂BF₄Cl₆: C, 46.61%; H, 3.49%; N, 5.71%. ¹H NMR (500 MHz, CDCl₃, δ): 7.71 (d, $J = 10$ Hz, (M/N(1H)), 7.69 (d, $J = 5$ Hz, K/L(1H)), 7.55–7.40 (m, overlapping signals, S/T(1H), Q/R(1H), O/P(2H), W/X(2H), K/L(1H)), 7.22–7.36 (m, overlapping signals, Y/Z(2H), S/T(1H), U/V(2H), Q/R(1H)), 7.19 (d, $J = 5$ Hz, M/N(1H)), 4.93 (d, $J = 15$ Hz, 1H, –CH₂–), 4.66 (t, $J = 7.5$ Hz, 1H, CH₂CH), 4.61 (d, $J = 0$ Hz, 1H, CCHC), 4.44 (s, 3H, CH₃), 4.11 (d, $J = 0$ Hz, 1H, CCHC), 3.93 (dd, 1H, $J = 10$ Hz, $J = 15$ Hz, 1H, –CH₂–), 3.84 (s, 3H, CH₃), 3.80 (dd, $J = 10$ Hz, $J = 15$ Hz, 1H, –CH₂–), 2.24 (d, $J = 15$ Hz, –CH₂–), 1.97 (t, $J = 10$ Hz, 1H, CH₂CH). ¹³C{¹H} NMR (75 MHz, CDCl₃, δ): 186.32 (d, $J = 34$ Hz, A/B), 185.57 (d, $J = 34$ Hz, A/B), 179.96 (d, $J = 45$ Hz, C/D), 179.93 (d, $J = 45$ Hz, C/D), 144.12 (s, O/P), 143.52 (s, O/P), 138.17 (s, Q/R), 137.97 (s, Q/R), 135.03 (s, i/j), 134.70 (s, i/j), 134.59 (s, k/l), 133.87 (s, k/l), 127.15 (s, Y/Z), 127.12 (s, Y/Z), 126.77 (s, W/X), 126.71 (s, W/X), 125.75 (s, c/d), 125.40 (s, e/f), 125.03 (s, g/h), 124.93 (s, e/f), 124.82 (s, g/h), 124.73 (s, c/d), 123.98 (s, a/b), 122.52 (s, a/b), 111.92 (s, U/V), 111.72 (s, U/V), 110.65 (s, S/T), 109.91 (s, S/T), 54.88 (s, K/L/M/N), 51.93 (s, K/L/M/N), 49.71 (s, I/J), 47.12 (s, G/H), 46.77 (s, G/H), 45.13 (s, I/J), 37.70 (s, E/F), 36.17 (s, E/F). For a legend to the NMR assignment see ESI.† MS(HR-ESI-FTICR+): Calc. for [C₃₆H₃₀N₄RhO₂]⁺: m/z 653.1418 M⁺, Found m/z 653.1348.

Catalytic hydrogenation of benzene

In an inert atmosphere, a spatula tip of catalyst (~5 mg) was added to a J-Young tube followed by approximately 1 mL of deuterated benzene. A freeze–pump–thaw method was then used to remove the nitrogen. Three cycles were performed before 1 atm of hydrogen was added *via* a Schlenk line. The reaction vessel was then placed in an oil bath at 50 °C for 24 h.

Catalytic hydrogenation of *trans*-methylstilbene⁸⁶

The catalysts, 3-R, 4-R or [Rh(nbd)₂](BF₄), and *trans*-methylstilbene (200 mg, 1.03 mmol) were dissolved in 5 mL of solvent. The resulting solution was transferred to a stainless steel Parr Instruments autoclave with a gauge block attachment in an inert atmosphere. The autoclave was filled and flushed

three times with hydrogen before it was finally pressurized with hydrogen (25–100 bar). The autoclave was heated to the desired temperature. After 24 h, the hydrogen was released. The solution was then filtered. The filtrate was removed *in vacuo* and a ¹H NMR spectrum was obtained in CDCl₃. Any precipitate that formed was extracted into DMSO-*d*₆ and a ¹H NMR spectrum obtained. The autoclave was cleaned with nitric acid between reactions to avoid contamination by any Rh⁰ and Ir⁰ that may have formed during the previous catalysis. Enantioselectivity was evaluated by HPLC analysis.

Catalytic hydrogenation of methyl-2-acetamidoacrylate⁸⁷

The catalyst, 3-R or 4-R, and methyl-2-acetamidoacrylate (200 mg, 1.40 mmol) were dissolved in 5 mL of solvent. The resulting solution was transferred to a stainless steel Parr Instruments autoclave with a gauge block attachment in an inert atmosphere. The autoclave was filled and flushed three times with hydrogen before it was finally pressurized to 50 bar of hydrogen. The autoclave was heated at 50 °C for the allotted time. After the allotted time, the hydrogen was released. The sample was then submitted to GC-MS to determine % conversion and % enantiomeric excess. The autoclave was cleaned with nitric acid between reactions to avoid contamination of Rh⁰ and Ir⁰ that may have formed during the previous catalysis. GC conditions: Alltech Chirasil-VAL (25 m × 0.25 mm × 16 μm), 40 °C isothermal for 1 min, followed by an increase of 10 °C min⁻¹ to 160 °C, $t(R) = 9.3$ min and $t(S) = 9.6$ min.

Catalytic hydrogenation transfer of methyl ketones⁶⁶

The catalyst, 3-diPh (2 mol%), KOH (5 mg, 0.089 mmol) and the methyl ketone (0.500 mmol) were dissolved in 2 mL of 2-propanol. The resulting solution was stirred at 70 °C. After 5 h the 2-propanol was removed *in vacuo*. The % conversion was determined by ¹H NMR spectroscopy and the ee by HPLC analysis. HPLC conditions: Diacel chiralpak IB column (250 × 4.6 mm id); 98 : 2 hexanes : 2-propanol; 212 nm; 0.5 mL min⁻¹; 1-phenylethanol: $t(S) = 10.7$ min and $t(R) = 12.2$ min; 1-(naphthalene-2-yl)ethanol: $t(R) = 46.5$ min and $t(S) = 48.8$ min; 1-(4-bromophenyl)ethanol: $t(R) = 27.3$ min and $t(S) = 28.6$; 1-(3-bromophenyl)ethanol: $t(R) = 25.9$ min and $t(S) = 27.3$ min.

Catalytic hydroformylation of styrene

The catalyst, 4-R or 5-Me and styrene (50 mg, 0.480 mmol) were dissolved in 1.5 mL of solvent. The resulting solution was transferred to a stainless steel Parr Instruments autoclave with a gauge block attachment in an inert atmosphere. The autoclave was filled and flushed three times with syngas (1 : 1 CO : H₂) before it was finally pressurized to the desired pressure. The autoclave was heated at 50 °C. After 24 h, the pressure was released. The reaction mixture was analysed without further purification by GC. The autoclave was cleaned with nitric acid between reactions to avoid contamination of Rh⁰ that may have formed during the previous catalysis. GC conditions: Supleco Beta Dex 225 column, 100 °C isothermal for 5 min, followed by an increase of 4 °C min⁻¹ to 160 °C. Styrene, $t = 9$ min; 2-phenylpropionaldehyde (branched isomer), $t(S) = 18$ min and $t(R) = 18.2$ min; 3-phenylpropionaldehyde (linear isomer), $t = 22$ min.

X-Ray crystallographic study†

Data were collected at 173 K on a Siemens SMART PLATFORM equipped with a CCD area detector and a graphite monochromator utilizing Mo K α radiation ($\lambda = 0.71073 \text{ \AA}$). The structure was solved by the Direct Methods in SHELXTL6, and refined using full-matrix least squares. The non-H atoms were treated anisotropically, whereas the hydrogen atoms were calculated in ideal positions and were riding on their respective carbon atoms.

Acknowledgements

The authors thank the Camille and Henry Dreyfus Foundation and K. A. A. thanks the NSF and UF for funding the purchase of X-ray equipment. Research quantities of the DEAM-type ligands presented herein are now available for purchase from Strem Chemicals Inc.

References

- 1 F. A. Glorius, *N-Heterocyclic Carbenes in Transition Metal Catalysis*, Springer-Verlag, Berlin, Germany, 2007.
- 2 S. P. Nolan, *N-Heterocyclic Carbenes in Synthesis*, Wiley-VCH, Weinheim, Germany, 2006.
- 3 W. A. Herrmann, *Angew. Chem., Int. Ed.*, 2002, **41**, 1290.
- 4 L. H. Gade and S. Bellemin-Laponnaz, *Coord. Chem. Rev.*, 2007, **251**, 718.
- 5 E. A. B. Kantchev, C. J. O' Brien and M. G. Organ, *Angew. Chem., Int. Ed.*, 2007, **46**, 2768.
- 6 R. E. Douthwaite, *Coord. Chem. Rev.*, 2007, **251**, 702.
- 7 M. C. Perry and K. Burgess, *Tetrahedron: Asymmetry*, 2003, **14**, 951.
- 8 E. Peris and R. Crabtree, *Coord. Chem. Rev.*, 2004, **248**, 2239.
- 9 V. Dragutan, I. Dragutan and A. Demonceau, *Platinum Met. Rev.*, 2005, **49**, 123.
- 10 V. Dragutan, I. Dragutan, L. Delaude and A. Demonceau, *Coord. Chem. Rev.*, 2007, **251**, 765.
- 11 R. H. Grubbs, *Nobel Prize Lecture*, Stockholm, 2005.
- 12 R. H. Grubbs, *Handbook of Metathesis*, Wiley-VCH, Weinheim, Germany, 2003.
- 13 T. M. Trnka and R. H. Grubbs, *Acc. Chem. Res.*, 2001, **34**, 18.
- 14 M. Hechenroth, E. Kluser, A. Neels and M. Albrecht, *Angew. Chem., Int. Ed.*, 2007, **46**, 6293.
- 15 W. A. Herrmann, G. D. Frey, E. Herdtwick and M. Steinbeck, *Adv. Synth. Catal.*, 2007, **349**, 1677.
- 16 L. D. Vazquez-Serrano, B. T. Owens and J. M. Buriak, *Inorg. Chim. Acta*, 2006, **359**, 2786.
- 17 D. P. Allen, C. M. Crudden, L. A. Calhoun, R. Wang and A. Decken, *J. Organomet. Chem.*, 2005, **690**, 5736.
- 18 U. L. Dharmasena, H. M. Foucault, E. N. dos Santos, D. E. Fogg and S. P. Nolan, *Organometallics*, 2005, **24**, 1056.
- 19 D. Baskakov, W. A. Herrmann, E. Herdtweck and S. D. Hoffmann, *Organometallics*, 2007, **26**, 626.
- 20 D. P. Allen, C. M. Crudden, L. A. Calhoun and R. Wang, *J. Organomet. Chem.*, 2004, **689**, 3203.
- 21 L. D. Vazquez-Serrano, B. T. Owens and J. M. Buriak, *Chem. Commun.*, 2002, 2518.
- 22 H. M. Lee, T. Jiang, E. D. Stevens and S. P. Nolan, *Organometallics*, 2001, **20**, 1255.
- 23 H. M. Lee, D. C. Smith, Jr., Z. Ho, E. D. Stevens, C. S. Yi and S. P. Nolan, *Organometallics*, 2001, **20**, 794.
- 24 M. Dinger and J. C. Mol, *Eur. J. Inorg. Chem.*, 2003, 2827.
- 25 P. Csabai and F. Joo, *Organometallics*, 2004, **23**, 5640.
- 26 A. Corma, E. Gutierrez-Puebla, M. Iglesias, A. Monge, S. Perez-Ferreras and F. Sanchez, *Adv. Synth. Catal.*, 2006, **348**, 1899.
- 27 I. Kownacki, M. Kubiicki, K. Szubert and B. Marciniak, *J. Organomet. Chem.*, 2008, **693**, 321.
- 28 D. S. McGuinness, M. J. Green, K. J. Cavell, B. W. Skelton and A. H. White, *J. Organomet. Chem.*, 1998, **565**, 165.
- 29 D. S. McGuinness and K. J. Cavell, *Organometallics*, 2000, **19**, 4918.
- 30 C. M. Crudden and P. A. Allen, *Coord. Chem. Rev.*, 2004, **248**, 2247.
- 31 K. J. Cavell and D. S. McGuinness, *Coord. Chem. Rev.*, 2004, **248**, 671.
- 32 A. A. Danopoulos, N. Tsoureas, J. C. Green and M. B. Hursthouse, *Chem. Commun.*, 2003, 756.
- 33 L. C. Campeau, P. Thansandote and K. Fagnou, *Org. Lett.*, 2005, **7**, 1857.
- 34 W. J. Marshall and V. V. Grushin, *Organometallics*, 2003, **22**, 1591.
- 35 S. Caddick, F. G. N. Cloke, P. B. Hitchcock, J. Leonard, A. K. Lewis, D. McKercher and L. R. Titcomb, *Organometallics*, 2002, **21**, 4318.
- 36 D. S. McGuinness and K. J. Cavell, *Organometallics*, 1999, **18**, 1596.
- 37 H. van Rensburg, R. P. Tooze, D. F. Foster and A. M. Z. Slawin, *Inorg. Chem.*, 2004, **43**, 2468.
- 38 H. van Rensburg, R. P. Tooze, D. F. Foster and S. Otto, *Inorg. Chem.*, 2007, **46**, 1963.
- 39 A. M. Magill, B. F. Yates, K. J. Cavell, B. W. Skelton and A. H. White, *Dalton Trans.*, 2007, 3398.
- 40 F. Wu, V. K. Dioumaev, D. J. Szalda, J. Hanson and R. M. Bullock, *Organometallics*, 2007, **26**, 5079.
- 41 D. S. McGuinness, N. Saendig, B. F. Yates and K. J. Cavell, *J. Am. Chem. Soc.*, 2001, **123**, 4029.
- 42 D. S. McGuinness, K. J. Cavell and B. F. Yates, *Chem. Commun.*, 2001, 355.
- 43 D. C. Graham, K. J. Cavell and B. F. Yates, *Dalton Trans.*, 2006, 1768.
- 44 D. C. Graham, K. J. Cavell and B. F. Yates, *Dalton Trans.*, 2005, 1093.
- 45 D. C. Graham, K. J. Cavell and B. F. Yates, *Dalton Trans.*, 2007, 4650.
- 46 X. Cui and K. Burgess, *Chem. Rev.*, 2005, **105**, 3272.
- 47 K. Källström and P. G. Andersson, *Tetrahedron Lett.*, 2006, **47**, 7477.
- 48 S. Nanchen and A. Pfaltz, *Helv. Chim. Acta*, 2006, **89**, 1559.
- 49 S. Nanchen and A. Pfaltz, *Chem.–Eur. J.*, 2006, **12**, 4550.
- 50 E. Bappert and G. Helmchen, *Synlett*, 2004, **10**, 1789.
- 51 M. C. Perry, X. Cui, M. T. Powell, D. R. Hou, J. H. Reibenspies and K. Burgess, *J. Am. Chem. Soc.*, 2003, **125**, 113.
- 52 T. Focken, G. Raabe and C. Bolm, *Tetrahedron: Asymmetry*, 2004, **15**, 1693.
- 53 R. Hodgeson and R. E. Douthwaite, *J. Organomet. Chem.*, 2004, **690**, 5822.
- 54 H. Seo, H. Park, B. Y. Kim, J. H. Lee, S. U. Son and Y. K. Chung, *Organometallics*, 2003, **22**, 618.
- 55 J. Zhou, J. W. Ogle, Y. Fan, V. Banphavichit, Y. Zhu and K. Burgess, *Chem.–Eur. J.*, 2007, **13**, 7162.
- 56 R. H. Crabtree, *Acc. Chem. Res.*, 1979, **12**, 331.
- 57 M. S. Jelicic, K. A. Abboud, I. Ghivirgia and A. S. Veige, *Organometallics*, 2007, **26**, 5267.
- 58 The ^{13}C NMR spectrum for 1-diPh was reported in reference 59, but the synthesis was reported as “unpublished results”.
- 59 J. Elguero, R. M. Claramunt, R. Garceran, S. Julia, L. Avila and J. M. Del Mazo, *Magn. Reson. Chem.*, 1987, **25**, 260.
- 60 O. V. Starikova, G. V. Dolgushin, L. I. Larina, P. E. Ushakov, T. N. Komarova and V. A. Lopyrev, *Russ. J. Org. Chem.*, 2003, **39**, 1467.
- 61 K. L. Gibis, G. Helmchen, G. Huttner and L. Zsolnai, *J. Organomet. Chem.*, 1993, **445**, 181.
- 62 (a) Solvent molecules within the lattice were disordered and could not be modeled properly. The program SQUEEZE, a part of the PLATON package of crystallographic software, was used to calculate the solvent disorder area and remove its contribution to the overall intensity data. (a) SQUEEZE: P. van der Sluis and A. L. Spek, *Acta Crystallogr.*, 1990, **A46**, 194; (b) PLATON: A. L. Spek, *J. Appl. Crystallogr.*, 2003, **36**, 7.
- 63 W. A. Herrmann, D. Baskakov, E. Herdtweck, S. D. Hoffmann, T. Bunlaksananusorn, F. Rampf and L. Rodefeld, *Organometallics*, 2006, **25**, 2449.
- 64 T. Chen, X. G. Liu and M. Shi, *Tetrahedron*, 2007, **63**, 4874.
- 65 M. Karplus, *J. Am. Chem. Soc.*, 1963, **85**, 2870–2871.
- 66 C. H. Leung, C. D. Incarvito and R. H. Crabtree, *Organometallics*, 2006, **25**, 6099.
- 67 M. Viciano, E. Mas-Marza, M. Sanau and E. Peris, *Organometallics*, 2006, **25**, 3063.
- 68 D. M. Khravov, V. M. Lynch and C. W. Bielawski, *Organometallics*, 2007, **26**, 6042.
- 69 A. Fuerstner, M. Alcarazo, H. Krause and C. W. Lehmann, *J. Am. Chem. Soc.*, 2007, **129**, 12676.
- 70 W. Duan, M. Shi and G. Rong, *Chem. Commun.*, 2003, 2916.
- 71 Q. Xu, X. Gu, S. Liu, Q. Dou and M. Shi, *J. Org. Chem.*, 2007, **72**, 2240.
- 72 Y. Canac, C. Lepeht, M. Abdalilah, C. Duhayon and R. Chauvin, *J. Am. Chem. Soc.*, 2008, **130**, 8406.

- 73 S. Burling, S. Douglas, M. F. Mahon, D. Nama, P. S. Pregosin and M. K. Whittlesey, *Organometallics*, 2006, **25**, 2642.
- 74 J. A. Widegren and R. G. Finke, *J. Mol. Catal. A: Chem.*, 2003, **198**, 317.
- 75 P. J. Dyson, *Dalton Trans.*, 2003, 2964.
- 76 R. W. Simms, M. J. Drewitt and M. C. Baird, *Organometallics*, 2002, **21**, 2958.
- 77 R. Dorta, E. D. Stevens, C. D. Hoff and S. P. Nolan, *J. Am. Chem. Soc.*, 2003, **125**, 10490.
- 78 A. K. de K. Lewis, S. Caddick, F. G. N. Cloke, N. C. Billingham, P. B. Hitchcock and J. Leonard, *J. Am. Chem. Soc.*, 2003, **125**, 10066.
- 79 L. S. Ott, S. Campbell, K. R. Seddon and R. G. Finke, *Inorg. Chem.*, 2007, **46**, 10335.
- 80 A. S. Veige, *Polyhedron*, 2008, **27**, 3177.
- 81 *Rhodium Catalyzed Hydroformylation: Catalysis by Metal Complexes*, P. W. N. M. van Leeuwen and C. Claver, Springer, 2002.
- 82 C. Li, E. Widjaja, W. Chew and M. Garland, *Angew. Chem., Int. Ed.*, 2002, **41**, 3785.
- 83 P. J. Collier, J. A. Iggo and R. Whyman, *J. Mol. Catal. A: Chem.*, 1999, **146**, 149.
- 84 H. U. Blaser, H. P. Jalett, W. Lottenbach and M. Studer, *J. Am. Chem. Soc.*, 2000, **122**, 12675.
- 85 L. Xing, F. Du, J.-J. Liang, Y.-S. Chen and Q.-L. Zhou, *J. Mol. Catal. A: Chem.*, 2007, **276**, 191.
- 86 C. Hedberg, K. Källström, P. Brandt, L. K. Hansen and P. G. Andersson, *J. Am. Chem. Soc.*, 2006, **128**, 2995.
- 87 W. Zhang and X. Zhang, *J. Org. Chem.*, 2006, **72**, 1023.